



Volume XXIV 2021

ISSUE no.1

MBNA Publishing House Constanta 2021



Scientific Bulletin of Naval Academy

SBNA PAPER • OPEN ACCESS

Designing Unmanned Underwater Vehicles through Biomimicry

To cite this article: M. TANER and K. T. GÜRSEL, Scientific Bulletin of Naval Academy, Vol. XXIV 2021, pg.61-73.

Submitted: 04.05.2021

Revised: 15.06.2021

Accepted: 22.07.2021

Available online at www.anmb.ro

ISSN: 2392-8956; ISSN-L: 1454-864X

doi: 10.21279/1454-864X-21-I1-007

SBNA© 2021. This work is licensed under the CC BY-NC-SA 4.0 License

Designing Unmanned Underwater Vehicles through Biomimicry

M Taner¹ and K T Gürsel¹

¹Dokuz Eylül University, Institute of Marine Sciences and Technology,
Department of Naval Architect, Haydar Aliyev Boulevard, Nr.32; Inciraltı – Balçova
35340 Izmir, Turkey
(Corresponding author, e-mail: mesuttaner44@gmail.com)

Abstract. Research vessels or small craft equipped for the specific purposes lead geological, geophysical and oceanographic research both at the coastal and offshore areas for constructing and surveying the engineering projects such as offshore structures, undersea pipelines, harbours, oil and natural gas extraction plants from resources etc., which require extensive labourship. However, this research method applied entails very high costs and can also include risks for occupational safety and property due to the harsh weather conditions at sea. In addition, high precision measurements cannot always function from the sea surface during such research projects above-mentioned. Thus, unmanned underwater vehicles (UUVs) have been designed and produced intensively in the last two decades.

The aim of this study was to generate form design of a proper unmanned underwater surveying vehicle to be able to conduct research on the geological and geophysical structure of the sea bottom as well as oceanographic opinions. Therefore, computational fluid dynamics (CFD) analysis of the DARPA Suboff submarine model was created, and the validation of the results obtained in these analyses was provided with those of the experiments of this DARPA Suboff model performed by Liu and Huang [1]. After successful conformity of the simulations carried out using the commercial software STAR CCM+ (Simulation of Turbulent flow in Arbitrary Regions - Computational Continuum Mechanics, C++ based), the UUV forms were created by means of different way including biomimicry methodology. In this context, the models of a mature goose-beaked whale (*ziphius cavirostris*), a mature sperm whale (*physeter macrocephalus*) and two torpedo-shaped UUV models as well a hybrid model including parts of a whale and torpedo-forms with the same displacement were analysed, and the results obtained were discussed.

1. Introduction

Research ships are customarily used in constructing and surveying the engineering projects such as in oil and natural gas resources, offshore structures, undersea pipelines, harbors at both the coastal and offshore areas, which require systematic geological, geophysical and/or oceanographic research. These operations compulsory involve extensive human labourship. However, this method comprises many disadvantages such as increasing the costs of management and research, reducing the accuracy of measurements, prolongation of the research periods and increasing the risks to human life and property by executing the research by those vehicles due to the harsh weather conditions at sea. Hence in the last two decades, unmanned and/or autonomous underwater vehicles (UUVs/AUVs) have been developed in universities and research communities intensively. UUVs offer an important opportunity to measure and collect detailed oceanographic, geological, geophysical and seismic data in-situ in the depths of the seas and oceans [2].

In designing these vehicles, exact prognosis of the hull resistance of an UUV is the most fundamental factor in determining a specific range of power requirements and so operation route of a

vehicle [2]. The power consumption of the UUVs operating underwater is directly related to the form and location of the vehicles, since most of the power is spent in generating thrust for forward traveling and, contemporary, remaining on a constant depth.

Numerous articles have dealt with hydrodynamic characteristics of the UUVs and/or AUVs of which the following papers were selected, among others.

Myring used the data of the Royal Aviation Association in his study to confirm the numerical analysis results obtained for a series of hull forms [3]. In this case, a method has been developed to determine the resistance force that was affected by the form of a hull in the axial symmetric flow [2]. For the application of the method above-mentioned, it is sufficient to define the detailed hull geometry, free flow conditions and transition points.

The study of Karim et al. exhibited analyses by the finite volume method based on Reynolds Averaged Navier-Stokes (RANS) equations for the calculation of viscous friction [4]. Numerical analyses were carried out on an AUV model series named DREA consisting of six axially symmetrical hulls with a length / diameter (L/D) ratio varying between 4 and 10, and turbulent flow around and behind the hulls was simulated using the Shear Stress Transport $k-\omega$ turbulence model.

Fangxi et al. in their study determined the appropriate turbulence model for resistance estimations of AUVs with a typical Myring form using the CFD method [5]. Therefore, resistance analysis of three-dimensional viscous flow for the AUV models has been performed by solving RANS equations with different viscous models. As a result of the comparison made with the experimental results, it was concluded that the Shear Stress Transport $k-\omega$ turbulence model is the most suitable algorithm for resistance estimation to be applied.

The study of Allotta et al. discussed the methodologies adopted for the design of AUVs [6]. In addition, preliminary design criteria for vehicles and design procedures as well testing of the drive systems were explained. According to the expected performance and requirements of the THESAURUS project, typical features of an AUV were to include low viscous resistance properties and high maneuverability as well navigational capabilities.

The aim of the study of Won et al. was to determine the ideal design under various forms of AUVs with nozzles by means of CFD simulations [7]. In this context, various factors affecting the resistance force and propeller performance of the AUVs were examined to increase the efficiency of the propulsion system. To raise the performance of the CFD analysis Taguchi method was used.

Joung et al. in their study described a procedure that uses CFD analysis to determine the hull resistance of an AUV under development in a certain speed range given [8]. The results of the CFD analysis revealed the distribution of velocity and pressure field etc. on the AUV hull and its propeller. Further, a methodology was presented to optimize the AUV profile to reduce its total resistance.

The aim of this study is to develop an unmanned underwater vehicle to carry out research on the geological and geophysical structure of the sea up to the deep of 1,000 m and on the Earth's layers as well oceanographic opinions, with the maximum and service speed in operation 8 kn and 2-3 kn, respectively.

For predicting the hull resistance of the UUV form to be designed, first the well-known examinations on DARPA Suboff model were investigated elaborately ([1],[9],[10]), and this model was analyzed through the commercial software STAR CCM+ (Simulation of Turbulent flow in Arbitrary Regions - Computational Continuum Mechanics, C++ based). Then the analysis results obtained were validated by the physical towing tank tests given in [11]. Subsequently, three UUV forms were generated by means of certain torpedo-shapes and biomimicry methodology. Further, two different whale types were modelled. To determine the optimum UUV form, all models generated were analyzed numerically.

2. Materials and Method

Many different methods can be used to develop the form of an UUV. Undoubtedly, the most effective of these is to use built submarine designs with present test results preferably. However, it is possible to make the design much more effective by using the biomimicry methodology.

The forms of the UUVs examined in this study were partially developed by the biomimicry methodology. Banger defines the concept of the biomimicry in his article as follows: "Biomimicry examines the functioning, models, systems, processes and components of the nature to get inspiration

(and sometimes to imitate) for the solution of engineering problems. As a result of these investigations, it tries to find clues for new solutions” [12].

This new UUV design must acquire superior maneuverability properties like a ROV, while it must keep the typical properties of an AUV [6]. Objects moving in a viscous liquid encounter viscous drag, which consists of two components: viscous pressure and frictional resistance depending both upon the Reynolds number. Therefore, it is very important that unmanned underwater vehicles have a suitable hydrodynamic form and surface properties.

The CFD method to be applied in all the simulations in this study was essentially validated by means of the test results of DARPA (Defence Advanced Research Projects Agency) Suboff Submarine boat selected which is often used for confirming the results of the CFD analyses carried out regarding UUVs (Fig. 1), since DARPA has also a typical AUV form of which test results are present. Therefore, the DARPA submarine was modelled exactly and analyzed by means of the software STAR CCM+ (Fig. 2-5) [9]. Figure 2 shows the model of the DARPA Suboff submarine, whilst Figures 3 and 4 exhibit the domain of this system analyzed and the meshed model, respectively. As a validation, Figure 5 indicates a good agreement of the results of the CFD analysis conducted in this study and those of the experiments of this submarine model carried out by Takahashi and Sahoo [9].

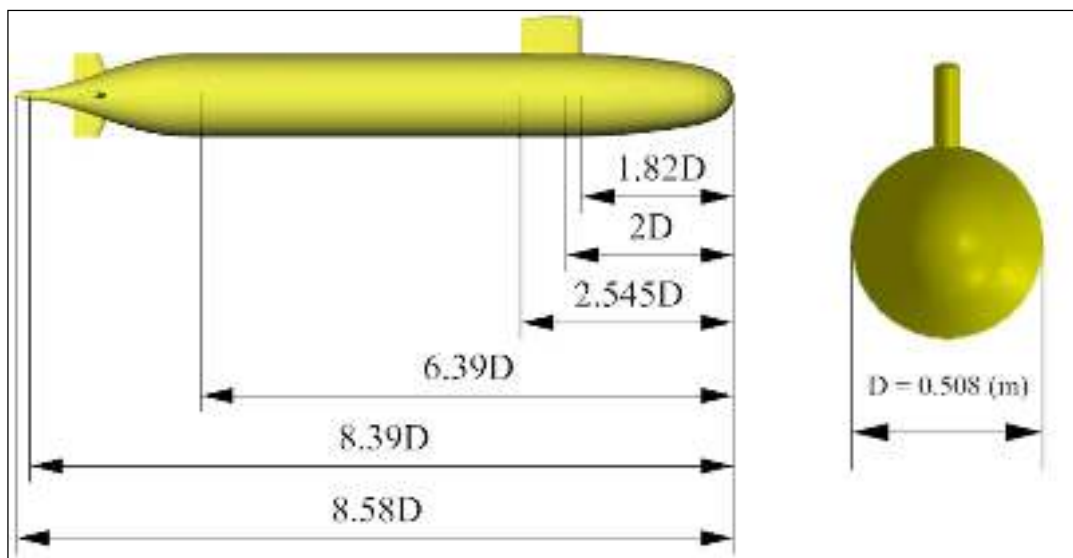


Figure 1. DARPA Suboff submarine model [13]



Figure 2. Modelled DARPA Suboff submarine hull

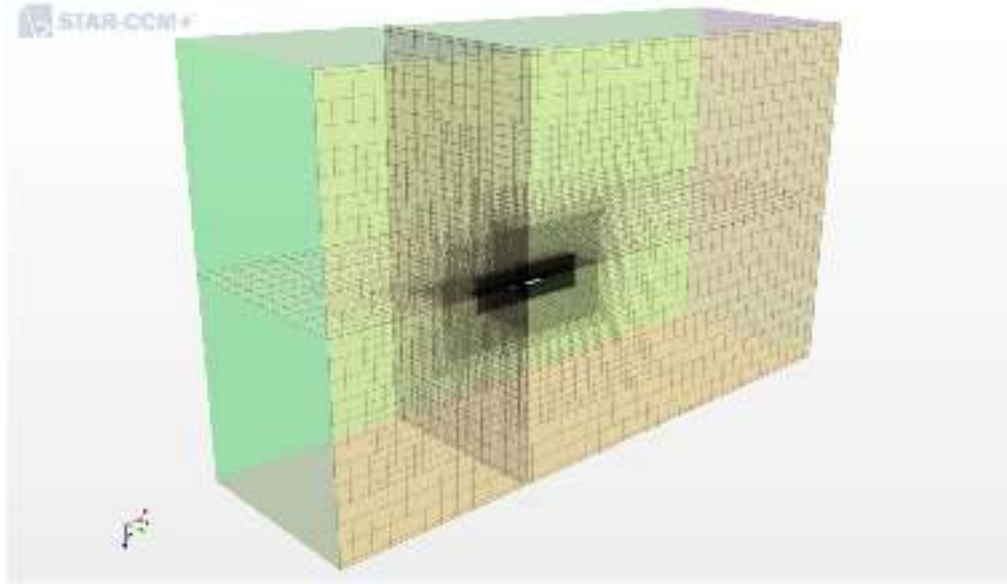


Figure 3. Domain of the DARPA Suboff submarine hull

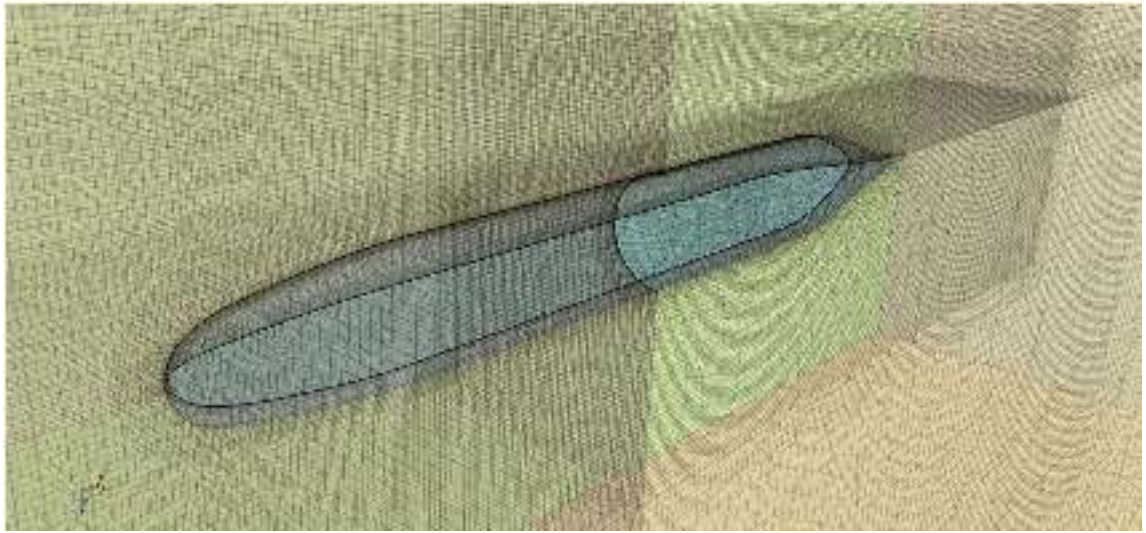


Figure 4. Meshed model of the DARPA Suboff hull

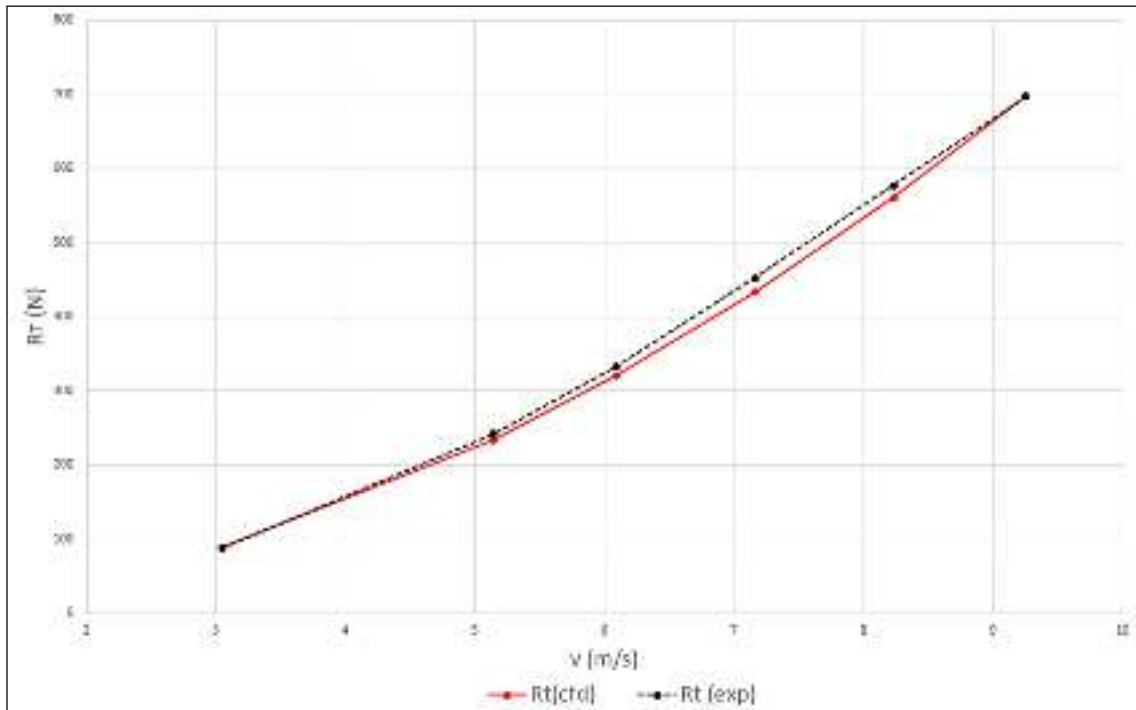


Figure 5. Total resistance results of the test and CFD analysis of the DARPA Suboff submarine

For utilizing the biomimicry methodology in this study, the models of a mature sperm whale (*physeter macrocephalus*) and a mature goose-beaked whale (*ziphius cavirostris*) have been created, since these whales can dive up to the deep of 3,000 m as given in Fig. 6 and 7, respectively. Furthermore, beaked and sperm whales can reach a top speed of 11-12 km/h and 35-45 km/h in submerged case, respectively.

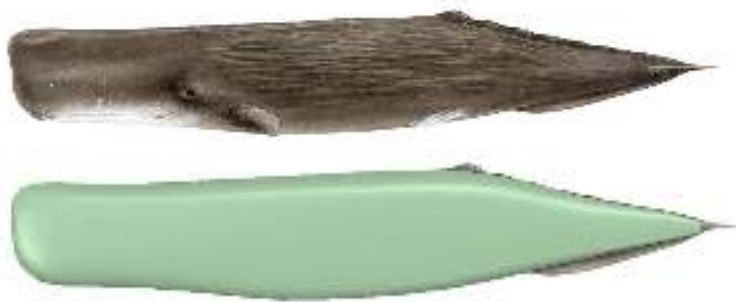


Figure 6. Modelling process of a sperm whale (*Physeter Macrocephalus*)

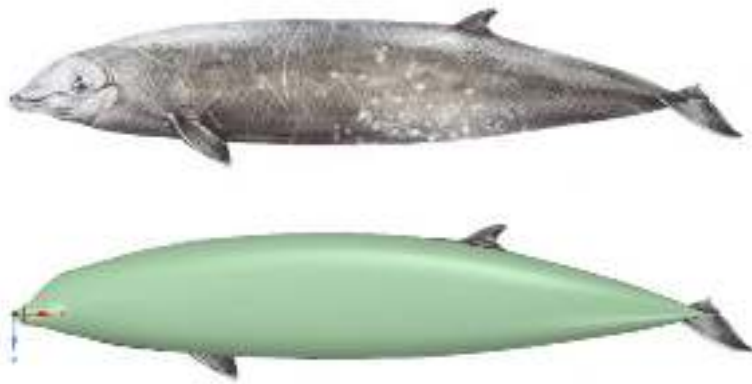


Figure 7. Modelling process of a beaked whale (*Ziphius Cavirostris*)

Further, two UUV forms were modelled, which were partially similar to the both hulls of the sperm and beaked whales, namely UUV-1 with sphere head and UUV-2 with ellipsoid head and slenderer stern, respectively (Fig. 8 and 9). As last, the head part of a mature beaked whale was taken out and the ellipsoid head of the UUV-2 was joined with the rest body of this whale without head part (Fig. 10). Thus, this hybrid model was developed principally with two aims. First, it was able to increase the model volume of the beaked whale, secondly, it was simpler to produce that model form.



Figure 8. Modeling of the UUV-1



Figure 9. Modeling of the UUV-2

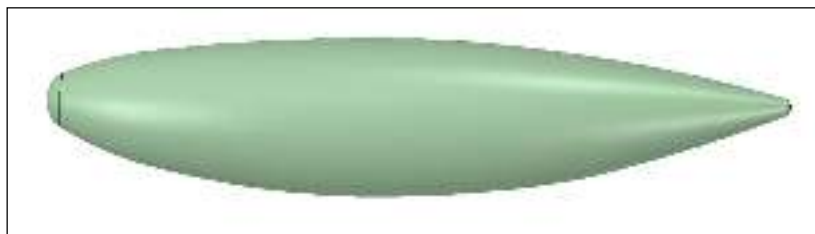


Figure 10. Creating of the hybrid model

Figures 11-16 indicate the domains of all models created in which they were analysed. Thus, it became possible to hydrodynamically compare the UUV forms shaped according to torpedoes and two whale forms generated by means of the biomimicry methodology, which were in fact evolved after millions of years as well a hybrid form each other. Therefore, it is assumed that all models of the UUVs and the whales as well the combination of both shall have an optimum speed of 5 m/s (18 km/h = 9,72 kn) to be able to compare all models each other [14][15].

After generating the models of two whales, a hybrid model and two torpedo shaped UUV ones, they had been meshed as given in Figures 6-16. Detailed CFD analyses of these models with the same volumic displacement of 5 m³ were conducted under the same conditions using the commercial software STAR CCM+ elaborately (Table 1).

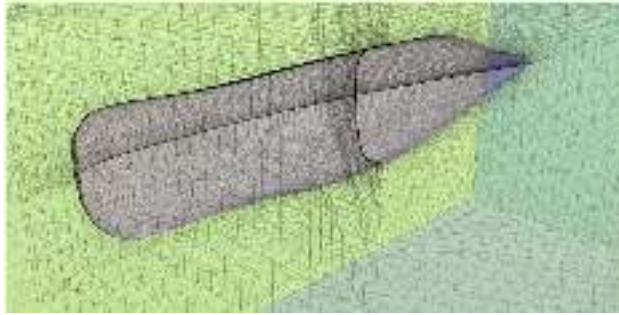


Figure 11. Meshed model of the sperm whale

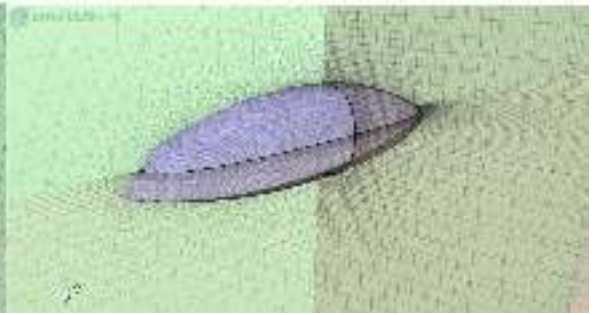


Figure 12. Meshed model of the beaked whale

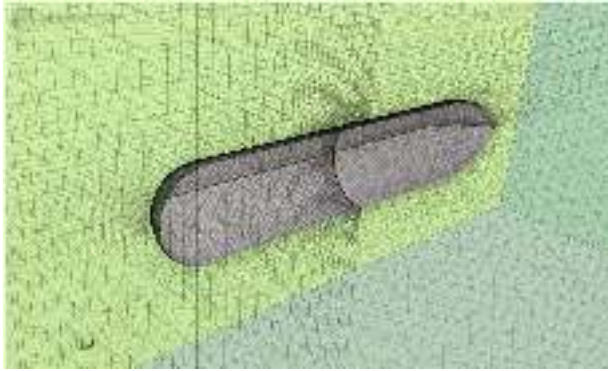


Figure 13. Meshed model of the UUV-1

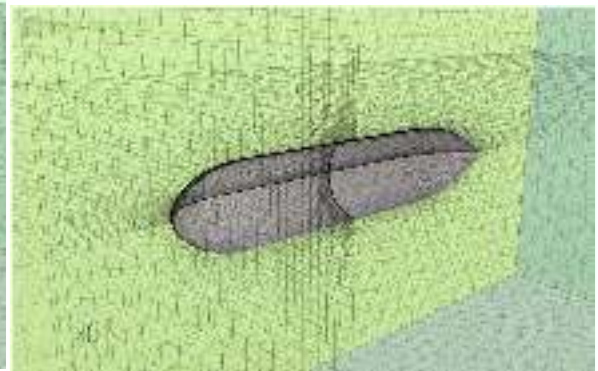


Figure 14. Meshed model of the UUV-2

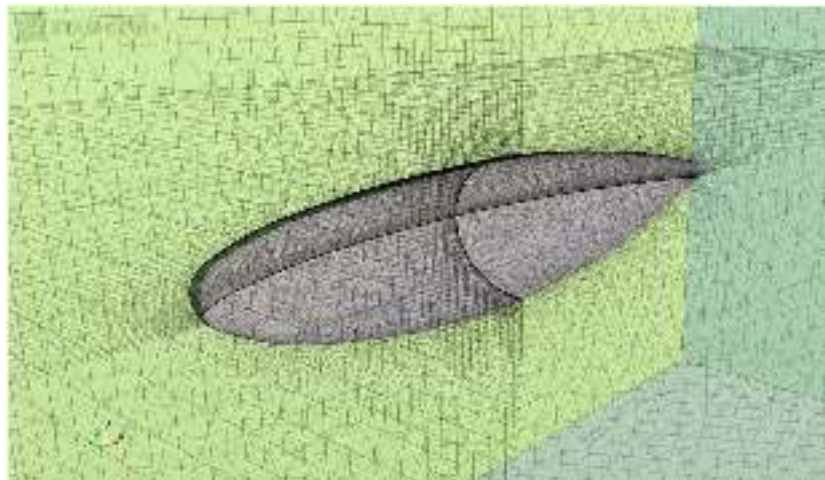


Figure 15. Meshed model of the hybrid

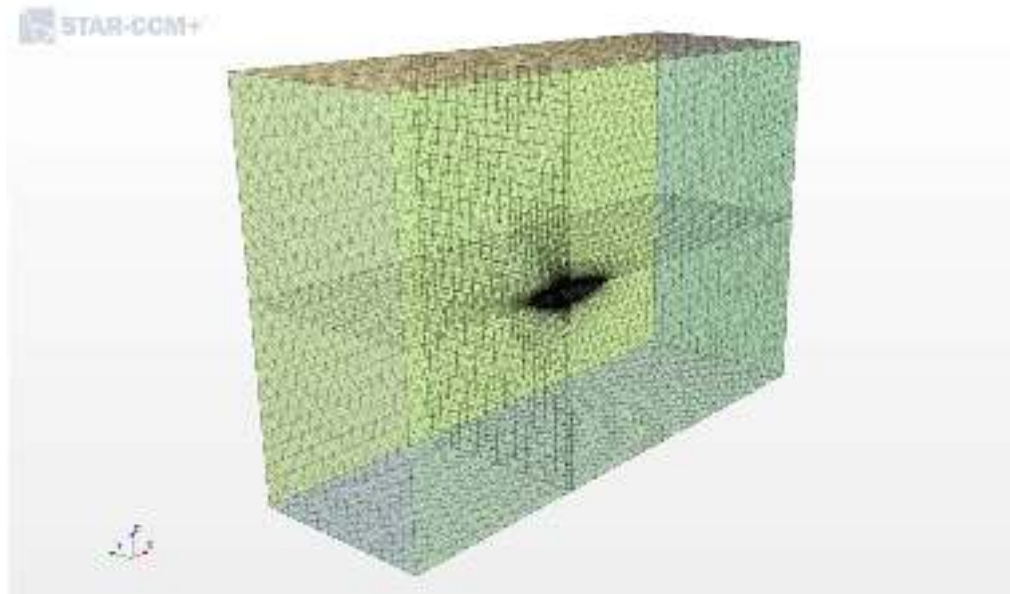


Figure 16. Domain of meshed hybrid model

Table 1. Origin of the created models

Name of Models	Models	Source of forming
Beaked whale		Itself
Sperm whale		Itself
UUV-1		Torpedo-shaped form with sphere head
UUV-2		Torpedo-shaped form with ellipsoid head and slenderer stern
HUUV		Beaked whale with ellipsoid head

3. Analysis of the Models and Results

3.1. CFD method formulation

This study investigates the resistance properties of UUVs with different forms by means of a commercial CFD solver STAR CCM+. Due to the complex behaviour of turbulence originating from its chaotic nature, time averaged values of corresponding parameters should be set into the equation that is called Reynolds Averaged Navier-Stokes Equation (RANSE), and time averaged equations of Navier - Stokes and continuity create the equation in tensorial notation as given in Eq. 1, which this software uses.

$$\rho \frac{D\bar{u}_i}{Dt} = F_i - \frac{\partial \bar{p}}{\partial x_i} + \mu \nabla^2 \bar{u}_i - \rho \left[\frac{\partial \bar{u}'_i \bar{u}'_j}{\partial x_j} \right] \quad (1)$$

In this research, the flow is assumed to be steady and incompressible. In CFD analyses of those UUV models treated in the section below, the turbulence modelling of “Shear Stress Transport k- ω algorithm (SSTKW) in the software STAR CCM+ was applied. The motive to selecting this modelling is that it generally predicts accurately the onset and the size of the flow separation under adverse pressure gradients on a floating and/or submerged rigid hull, since SSTKW model includes a modified turbulent viscosity formulation to calculate the transport effects of the principal turbulent shear stress, and the algorithm comprises a blending function that activates the standard k- ω model in the near-wall region and, however, the transformed k- ϵ model in the far-field zones [16][17]. The Shear Stress Transport k- ω model is a two-equation turbulence model as shown in Equations. 2 and 3:

$$\frac{\partial}{\partial t} (\rho k) + \frac{\partial}{\partial x_i} (\rho k u_i) = \frac{\partial}{\partial x_j} \left(\Gamma_k \frac{\partial k}{\partial x_j} \right) + G_k - Y_k + S_k \quad (2)$$

$$\frac{\partial}{\partial t} (\rho \omega) + \frac{\partial}{\partial x_i} (\rho \omega u_i) = \frac{\partial}{\partial x_j} \left(\Gamma_\omega \frac{\partial \omega}{\partial x_j} \right) + G_\omega - Y_\omega + D_\omega + S_\omega \quad (3)$$

Where mean:

k: Turbulence kinetic energy

ω : Specific dissipation rate

ρ : Density

G_k : Generation of turbulence kinetic energy

G_ω : Generation of specific dissipation rate

Γ_k : Effective diffusivity of k

Γ_ω : Effective diffusivity of ω

S_k ve S_ω : User defined source terms

Y_k ve Y_ω : Dissipation of k and ω due to turbulence

D_ω : Cross-diffusion term

Depending on the selected turbulence model, meshing the domains of all the models should be performed correspondingly. Thus, a layered grid near all the models was generated to obtain more accurate results, in which “trimmed hexahedral cell shape-based core mesh” was used. In the outer region, the larger mesh grid of the same type was implemented (Fig. 11-16). It should be mentioned that the turbulence models conducted usually work a certain range of the wall function y^+ , whose expanded form is given in Eq. 4.

$$y^+ = \frac{\rho y \sqrt{\frac{\mu}{\rho} \left(\frac{\partial u}{\partial y} \right)_{y=0}}}{\mu} \quad (4)$$

To indicate the wall function values y^+ obtained in mesh structures during the prediction of resistance analyses of the DARPA Suboff model, the grid structure of the entire fluid domain and the distributions of the y^+ values were given in Figures 4 and 17, respectively. According to this, the variation range of the wall function y^+ in boundary layer of the DARPA Suboff submarine hull and all the models created were given in Fig. 17 and 18-22 for the velocity of 5 m/s, respectively, in which the values of y^+ range $0 < y^+ < 2.43$. These values obtained should be supposed as a very good approach for the acceptable quality of the boundary layer modelling, since the resistance simulation results obtained

in this study were approved with those of the towing tank tests of the DARPA Suboff model carried out by Liu and Huang [1] as given in Figure 5.

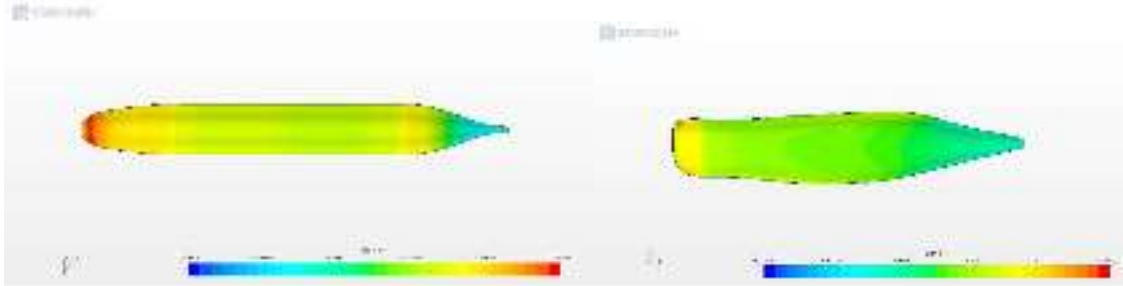


Figure 17. y^+ distribution of the DARPA model Figure 18. y^+ distribution of the sperm whale model

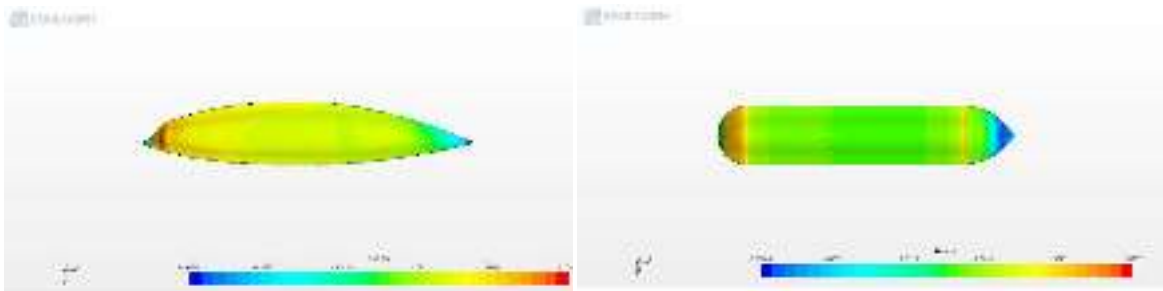


Figure 19. y^+ distribution of the beaked whale model Figure 20. y^+ distribution of the UUV-1 model



Figure 21. y^+ distribution of the UUV-2 model Figure 22. y^+ distribution of the HUUV model

3.2. Analysis of the developed models

Before all the five models created in the section above were analyzed numerically in which the turbulence modelling “Shear Stress Transport $k-\omega$ model (SSTKW-Menter) in STAR CCM+ was applied (Fig. 5-16), a successful validation of the CFD simulations applied in all analyses was provided by means of the test results of DARPA Suboff submarine model [1].

Considering the results of total viscous resistance of the whales obtained in the CFD analyses carried out by STAR CCM+ delivered interesting knowledge. Despite the different forms of both whales, they exhibited nearly the same viscous resistance values in full submerged state (Fig. 6,7,11,12,23), since they possessed relatively identical turbulent kinetic energy distribution fields at their hull surfaces (Fig. 24,25).

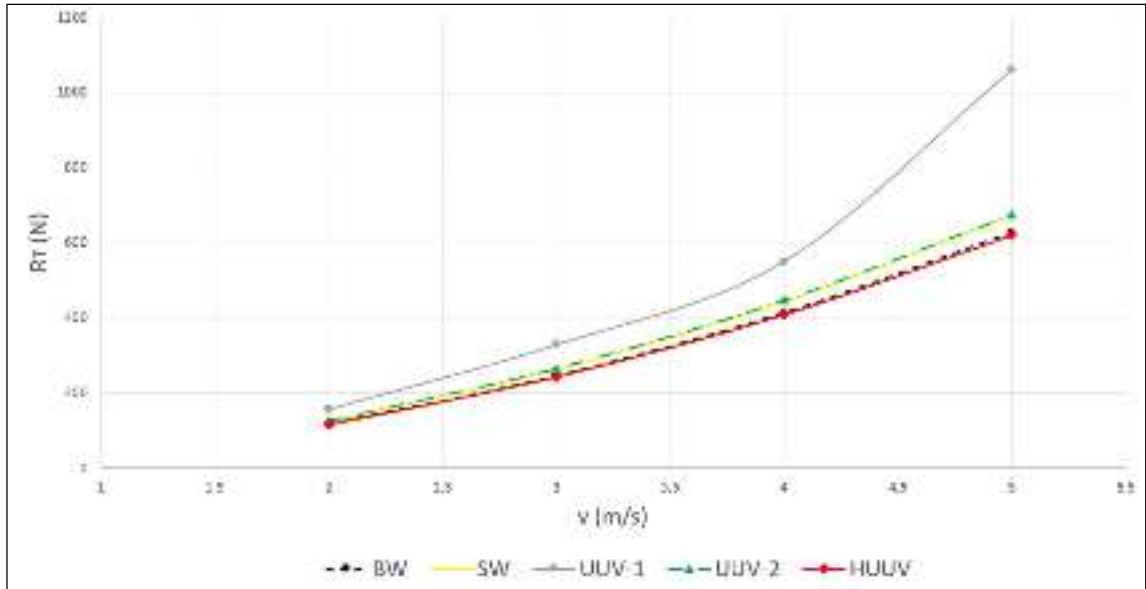


Figure 23. Total resistance results of the CFD analyses of all models

The results of the viscous resistance simulations performed on the UUV-1 were considerably higher than those of the other models (Fig. 23). The reason for that is the significantly higher level of the turbulent kinetic energy of this form (Fig. 26). The UUV-2 form with ellipsoid head experienced nearly the same resistance as the sperm whale (Fig. 23). The HUUV form exhibit the lowest level of viscous resistances as the form of the beaked whale as seen in Figures 23. These four models have similar turbulent kinetic energy distribution fields as expected (Fig. 24-28).

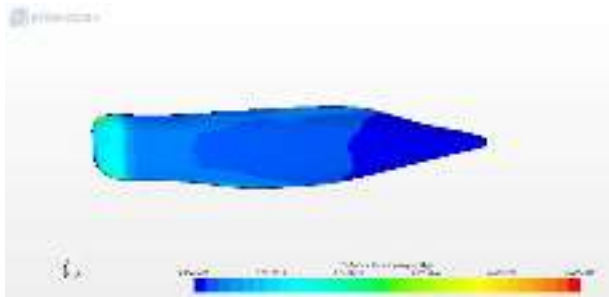


Figure 24. Turbulent kinetic energy distr. of sperm whale

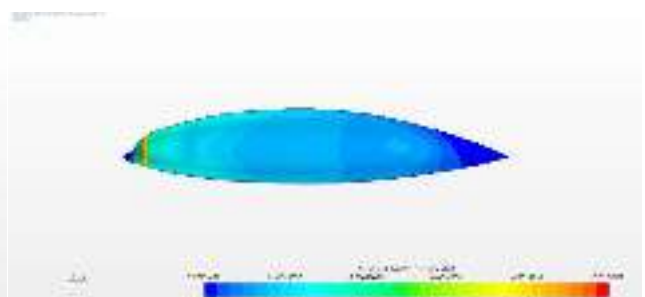


Figure 25. Turbulent kinetic energy distr. of beaked whale

In order to utilize the proper hydrodynamic characteristics of the form of the beaked whale, the hybrid model was created, namely HUUV as to further reduce the viscous resistance of the UUV-2: The bow part of this model consists of the one of the UUV-2 and its middle hull and stern are composed of the beaked whale without head part as seen in Figure 10. Additionally, the modification of the head part of this whale was to facilitate production methods of the form.

The total resistance of this hybrid form decreased about 10 % compared to the former form (UUV-2), and the distribution fields of the turbulent kinetic energy on this HUUV form improved considerably as seen in Fig. 23,27,28. It induces significantly less turbulences on the whole hull surface especially in the stern of the model than those in the aft hull of the models UUV-1 and UUV-2.

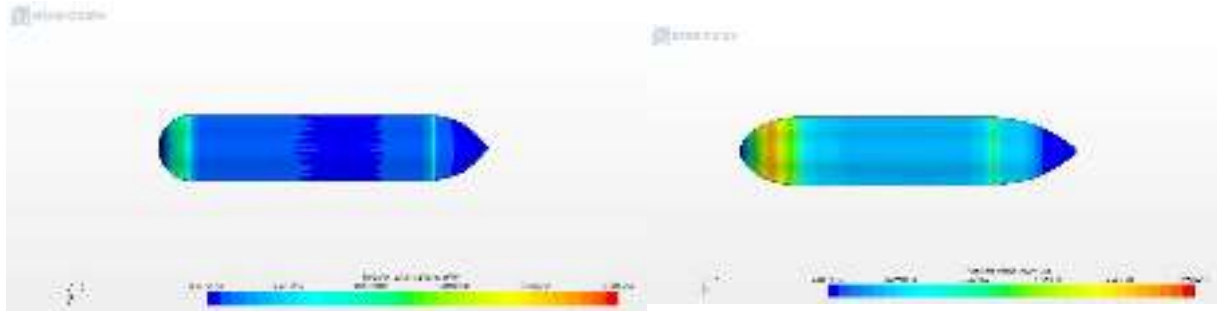


Figure 26. Turbul. kinetic en. distr. of the UUV-1 Figure 27. Turbul. kinetic en. distr. of the UUV-2

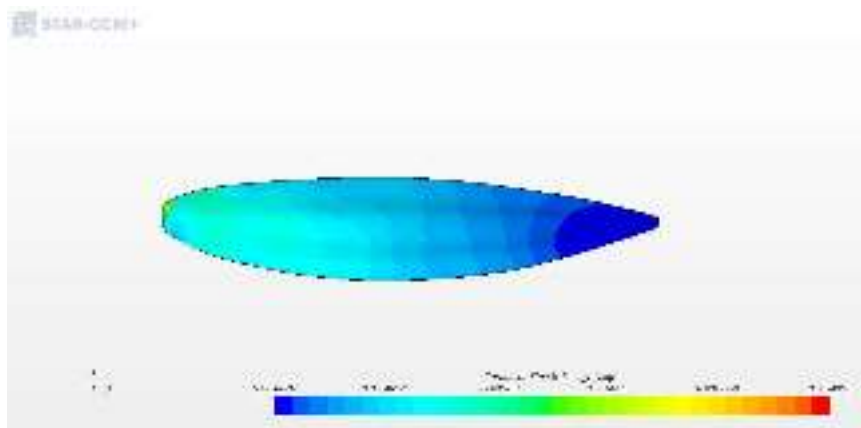


Figure 28. Turbulent kinetic energy distribution of the HUUV

4. Conclusions

This study was aimed to develop a proper form for an unmanned underwater vehicle to carry out investigations on the geological and geophysical structure of the sea bottom and on the Earth's mantle in seas as well oceanographic opinions. Therefore, to apply correctly the CFD method to the numerical simulations, the DARPA Suboff submarine boat was modelled and analyzed. After the results obtained in these CFD analyses had been validated through those of the experiments of the DARPA Suboff model performed by Liu and Huang [1], the simulations carried out on the generated models of a mature goose-beaked whale (*ziphius cavirostris*), a mature sperm whale (*physeter macrocephalus*) and two torpedo-shaped UUV models as well a hybrid UUV model created by means of biomimicry methodology, were analyzed in the same manner using the commercial software STAR CCM+, which had the same volumic displacement. The results obtained were investigated and discussed elaborately.

The new HUUV form generated appear to have better resistance related characteristics than the UUV-1 and UUV-2 as well both whales. Nevertheless, the forms of the both whales evolved after millions of years exhibit to possess significantly better characteristics than ones of the models UUV-1. In our case of form design, while developing a form with low resistance properties is the first design priority, an interior volume suitable for placing the navigation and propulsion system as well equipment in the vehicle developed, is also a very important design parameter. Since the form of a mature beaked whale contains less volume than the form of the HUUV generated, the form designed appears to be considerably also better in terms of space requirements and production methods.

References

- [1] Liu, H. L., Huang, T. T. (1998). Summary of DARPA SUBOFF experimental program data. Naval Surface Warfare Center Carderock Div Bethesda Md Hydromechanics Directorate.
- [2] Gürsel, K.T., Taner, M., Ünsalan, D., Neşer, G., Altunsaray, E., Önal, M. (2017). Form Development and Validation of an Autonomous Underwater Vehicle, “Mircea cel Batran” Naval Academy Scientific Bulletin, Volume XX – Issue 1.
- [3] Myring, D.F. (1976). A Theoretical Study of Body Drag in Subcritical Axisymmetric Flow. *Aeronautical Quarterly*, 27(3), pp. 186–194.
- [4] Karim, M., Rahman, M., Alim, A. (2008). Numerical Computation of Viscous Drag for Axisymmetric Underwater Vehicles, *Jurnal Mekanikal* No. 26, 9 – 21.
- [5] Fangxi, S., Lianhong, Z., Zhiliang, W., Leping, W. (2011). On Resistance Calculation for Autonomous Underwater Vehicles. *Advanced Materials Research Vols. 189-193* pp 1745-1748.
- [6] Allotta, B., Pugi, L., Bartolini, F., Ridolfi, A., Costanzi, R., Monni, N., Gelli, J. (2014). Preliminary Design and Fast Prototyping of an Autonomous Underwater Vehicle Propulsion System, *Proceedings of the Institution of Mechanical Engineers Part M Journal of Engineering for the Maritime Environment* 229(3), DOI: 10.1177/1475090213514040.
- [7] Won, D. J., Kim, J., Kim, J. (2015). Design optimization of duct-type AUVs using CFD analysis. *Intelligent Service Robotics*, 8(4), 233-245.
- [8] Joung, T. H., Sammut, K., He, F., Lee, S. K. (2012). Shape optimization of an autonomous underwater vehicle with a ducted propeller using computational fluid dynamics analysis. *International Journal of Naval Architecture and Ocean Engineering*. 4:44-56.
- [9] Takahashi, K., Sahoo, P. K. (2019). Fundamental CFD Study on the Hydrodynamic Performance of the DARPA SUBOFF Submarine. In *ASME 2019 38th International Conference on Ocean, Offshore and Arctic Engineering*. American Society of Mechanical Engineers Digital Collection.
- [10] Toxopeus, S. (2008). Viscous-flow calculations for bare hull DARPA SUBOFF submarine at incidence. *International Shipbuilding Progress*, 55(3), 227-251.
- [11] Budak, G., Beji, S. (2016). Computational Resistance Analyses of A Generic Submarine Hull Form And Its Geometric Variants. *Journal of Ocean Technology*, 11(2).
- [12] Genc, M. (2013). *Nature, Art and Biomimetical Science*, Doctor of Arts Degree, Hacettepe University -Graduate School of Fine Arts.
- [13] Lin, Y. H., Li, X. C. (2020). The Investigation of a Sliding Mesh Model for Hydrodynamic Analysis of a SUBOFF Model in Turbulent Flow Fields. *Journal of Marine Science and Engineering*, 8(10), 744.
- [14] Naughton, D. (2012). *The Natural History of Canadian Mammals*, Published by University of Toronto Press, ISBN 078-1-4426-4483-0, p. 699.
- [15] <https://oceanwide-expeditions.com/to-do/wildlife/spermwhale>. (Access date: 14.03.2017)
- [16] Menter, F. (1994). Two-equation eddy-viscosity turbulence models for engineering applications. *AIAA Journal*, 1598-1605.
- [17] Gürsel, K.T., Taner, M. (2019). Hydrodynamic Potential Improvement of Pontoon Boats, *Naval Engineers Journal*, June 2019; No. 131-2.